Supplementary Figures and Tables

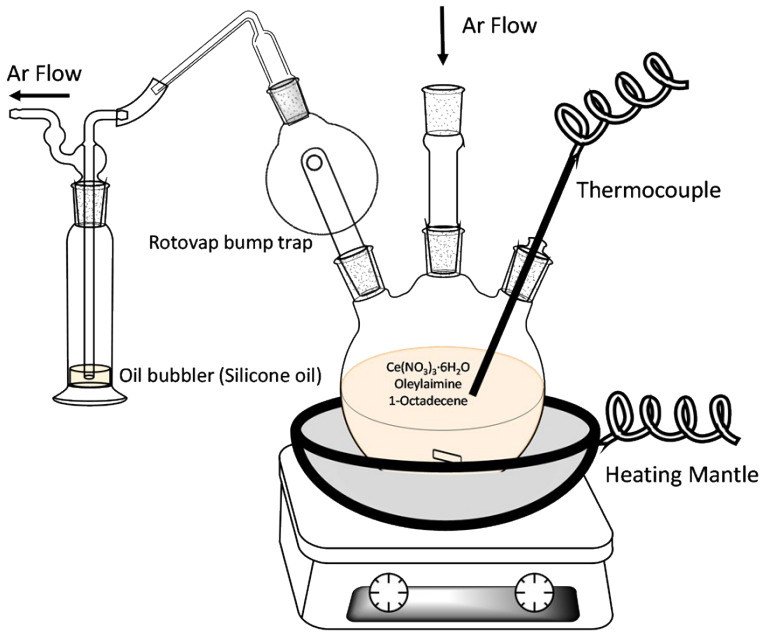

Scheme S1. Equipments designed for ceria nanoparticle thermodecomposition synthesis. An inert gas (Ar) is used to protect the reactions.

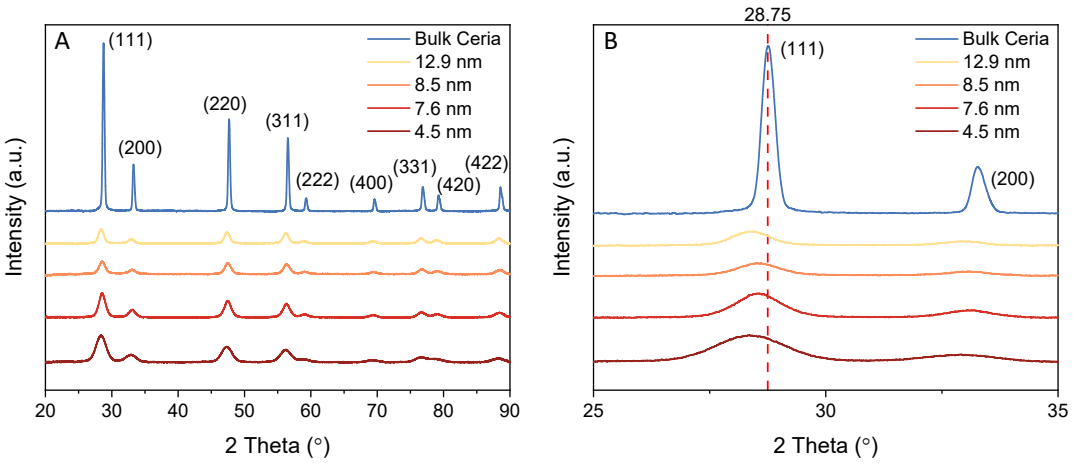

Figure S1. X-ray diffraction patterns of face-centered cubic (FCC) ceria powder (Aldrich, <5μm) and ceria nanoparticles with diameters of 4.5nm, 7.6nm, 8.5nm, 12.9nm as determined by TEM. Peak (2θ ~ 28.75°) broadening suggests that crystallite size decreases based on the Scherrer equation.

Table S1. Lattice parameter (LP), average grain size (D), and interplanar spacing (d-spacing) of ceria powder (Aldrich, <5µm) and ceria nanoparticles with diameters of 4.5nm, 7.6nm, 8.5nm, 12.9nm. Note the labels on the particles given on the right column correspond to the diameters found from the sizing of particles from electron microscopy data. The average grain size was calculated with the help of the Scherrer equation from line broadening, fixed with instrumental broadening obtained from the FWHM of bulk material. The d-spacing was calculated by the Bragg equation, and LP was calculated by a standard cubic indexation method using the angular position of the most prominent peak (111). Note the error on the grain size found from the XRD linewidths was calculated with a .10 degree error in the FWHM determination and a 10% error in the K constant due to departures from spherical particles.

Diameter TEM (nm)	d-spacing (Å)	LP (nm)	Grain Size (nm)	Error (nm)
4.5nm	3.145	0.545	6.04	0.12
7.6nm	3.130	0.542	9.16	0.14
8.5nm	3.124	0.541	9.90	0.15
12.9nm	3.120	0.540	11.73	0.16
Bulk Material	3.105	0.538	--	

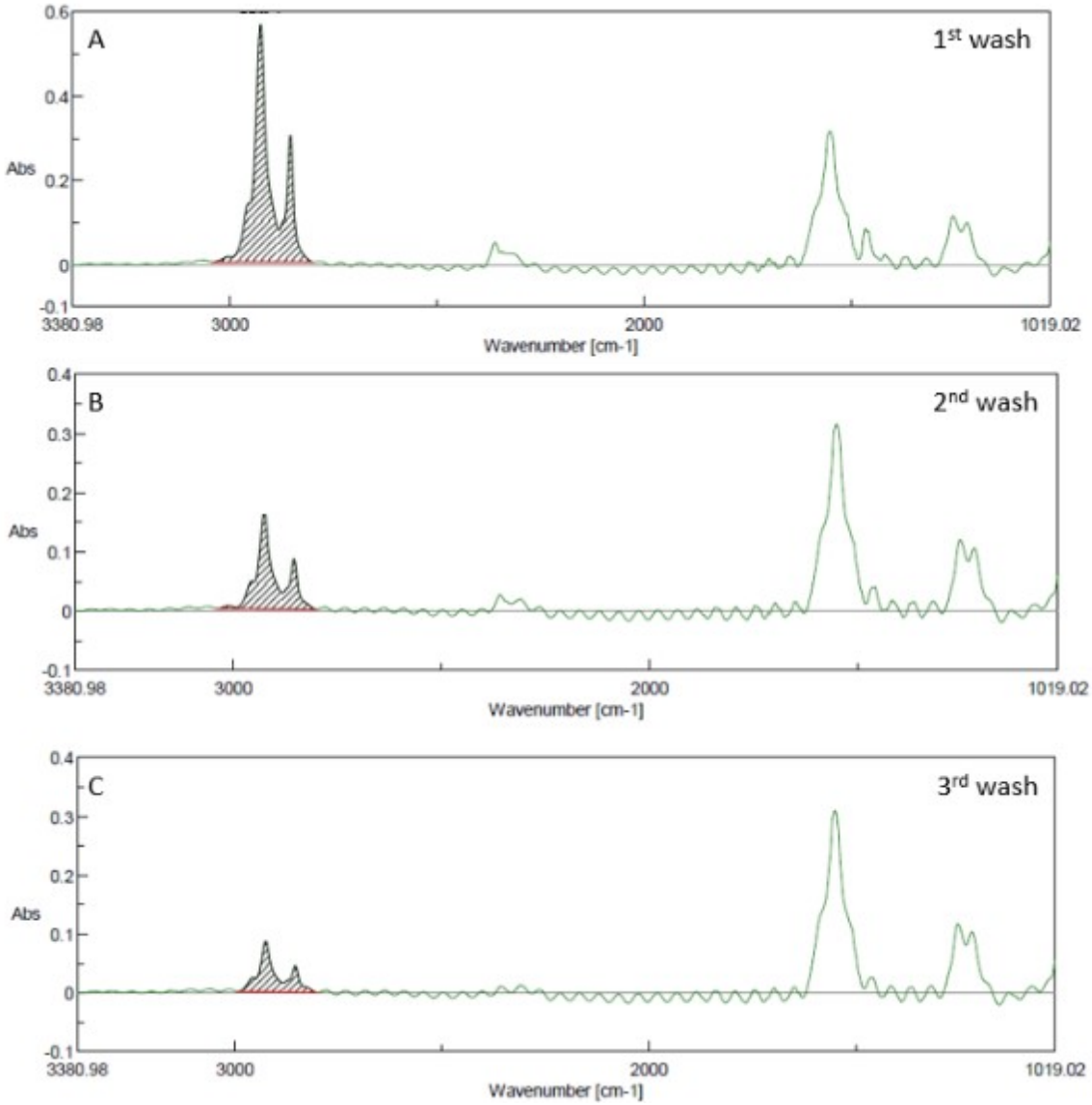

Figure S2. Fourier-transform infrared spectroscopy (FTIR) spectra of oleylamine coated ceria nanoparticle after purification: the first (A), second (B), and third (C) wash. One wash means nanoparticles were precipitated in acetone and methanol (1:1), then the sediment was collected by centrifugation (9000 rpm, 15 mins) and was redispersed in CCl_4. The shaded peak is the C-H stretch peak, and the area under the curve (AUC) is used to analyze the oleylamine concentrations on the surface of ceria nanoparticles.

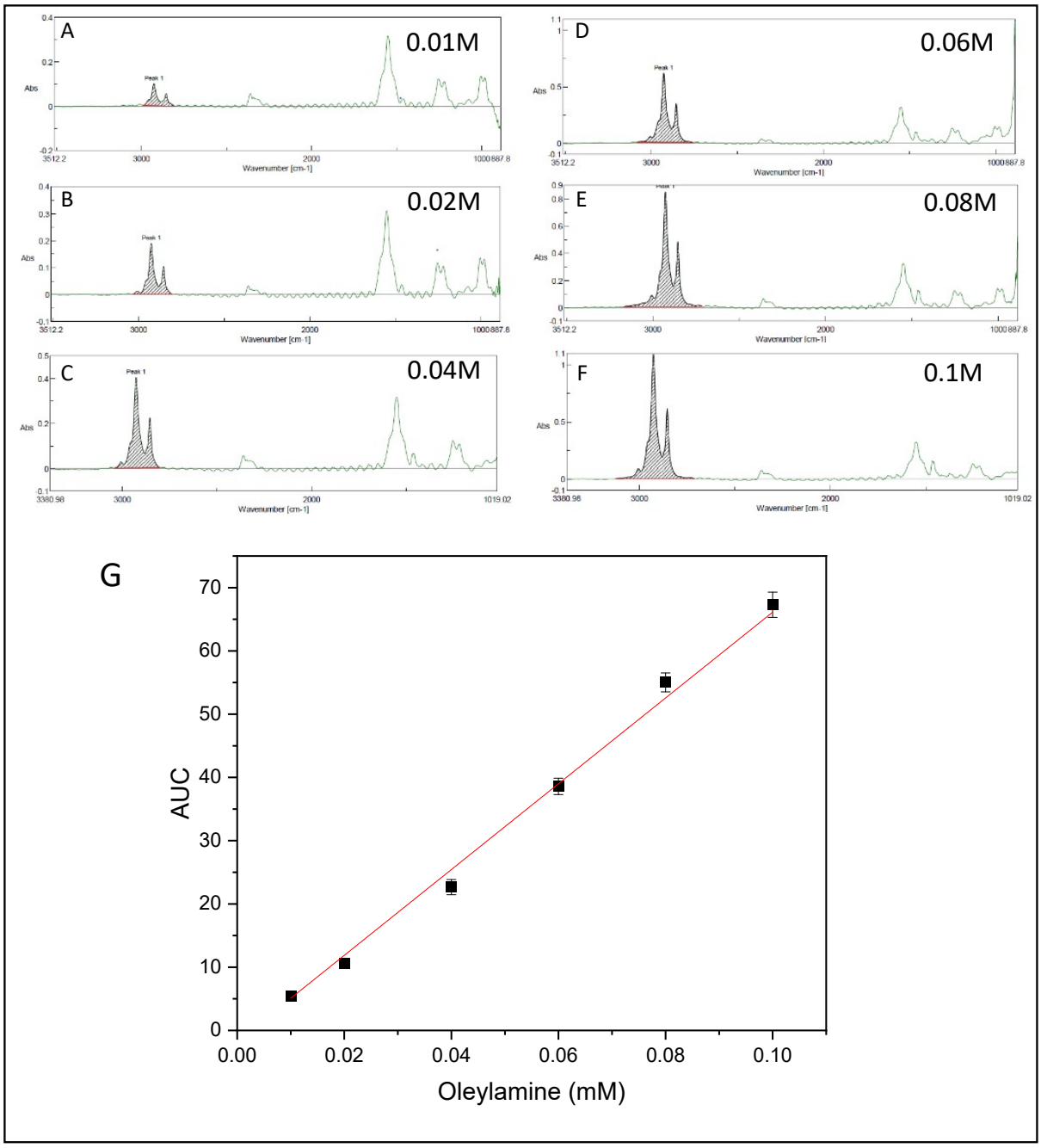

Figure S3. (A-F) Fourier-transform infrared spectroscopy (FTIR) spectra of oleylamine in CCl_4. The numbers on the top right corner suggest the concentrations of oleylamine. The shaded peak is the C-H stretch peak, and the area under the curve (AUC) is used for the calibration of oleylamine concentration in CCl_4. (G) Calibration line of oleylamine AUC of C-H stretch peak to the concentration.

Table S2. Oleylamine remaining on the surface of ceria nanoparticles (d ~ 4.5 nm) after each wash determined by C-H stretching peaks in FTIR spectra. Ceria nanoparticles were precipitated by acetone and methanol, then centrifuged and redispersed in CCl_4 for FTIR measurement.

	Area of the C-H stretch peak	Oleylamine (mol/L)	Oleylamine in solution per Nanoparticle	Estimated Oleylamine on Nanoparticle
Original sample	181.91	0.290	11666	200 - 400
Washed once	28.91	0.049	3574	
Washed twice	9.25	0.018	757	
Washed three times	4.74	0.010	263	

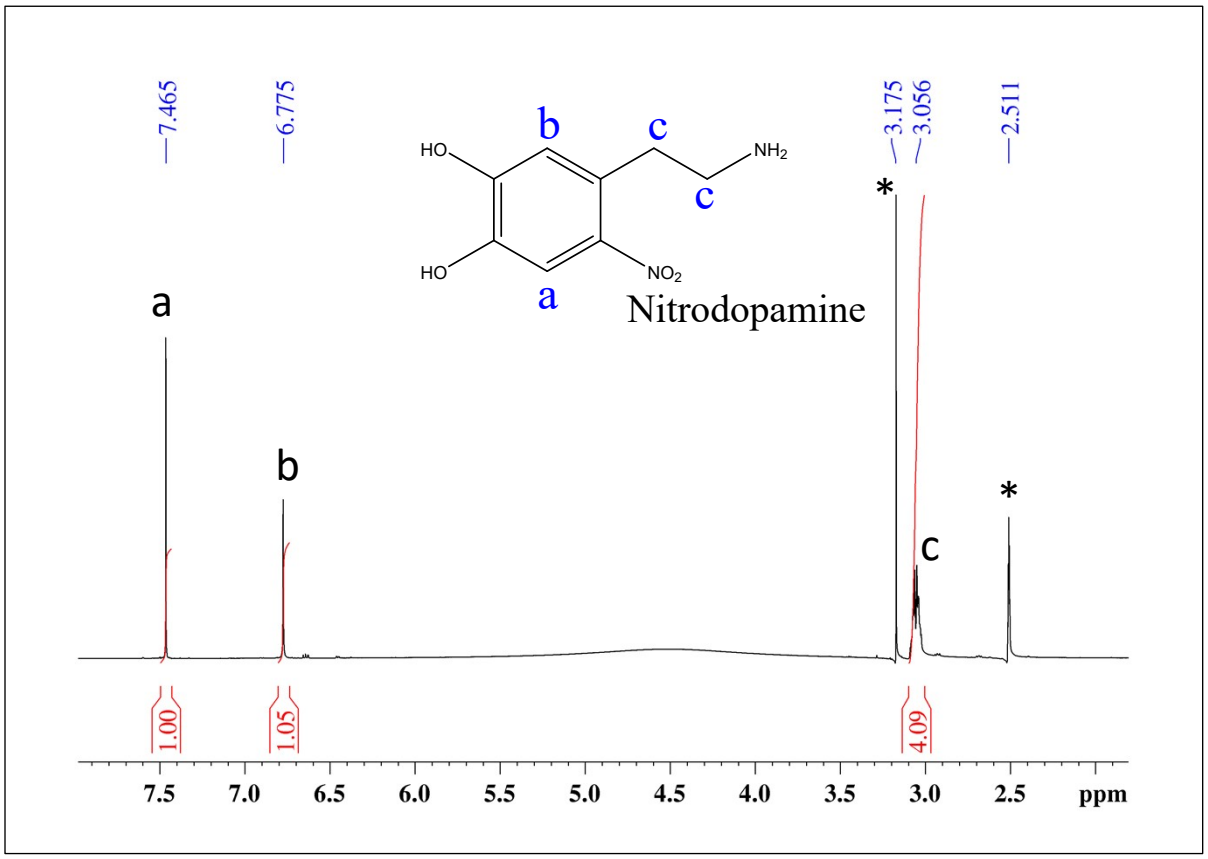

Figure S4. ^{1}H-NMR spectrum of nitrodopamine in DMSO-d_6. The peak(a) and peak(b) above 6.5 ppm represent protons on the dopamine aromatic ring. The peak(c) around 3 ppm represents protons on C-H chains. Peaks labeled with (*) suggest DMSO-d_6 solvent residual and HOD peaks.

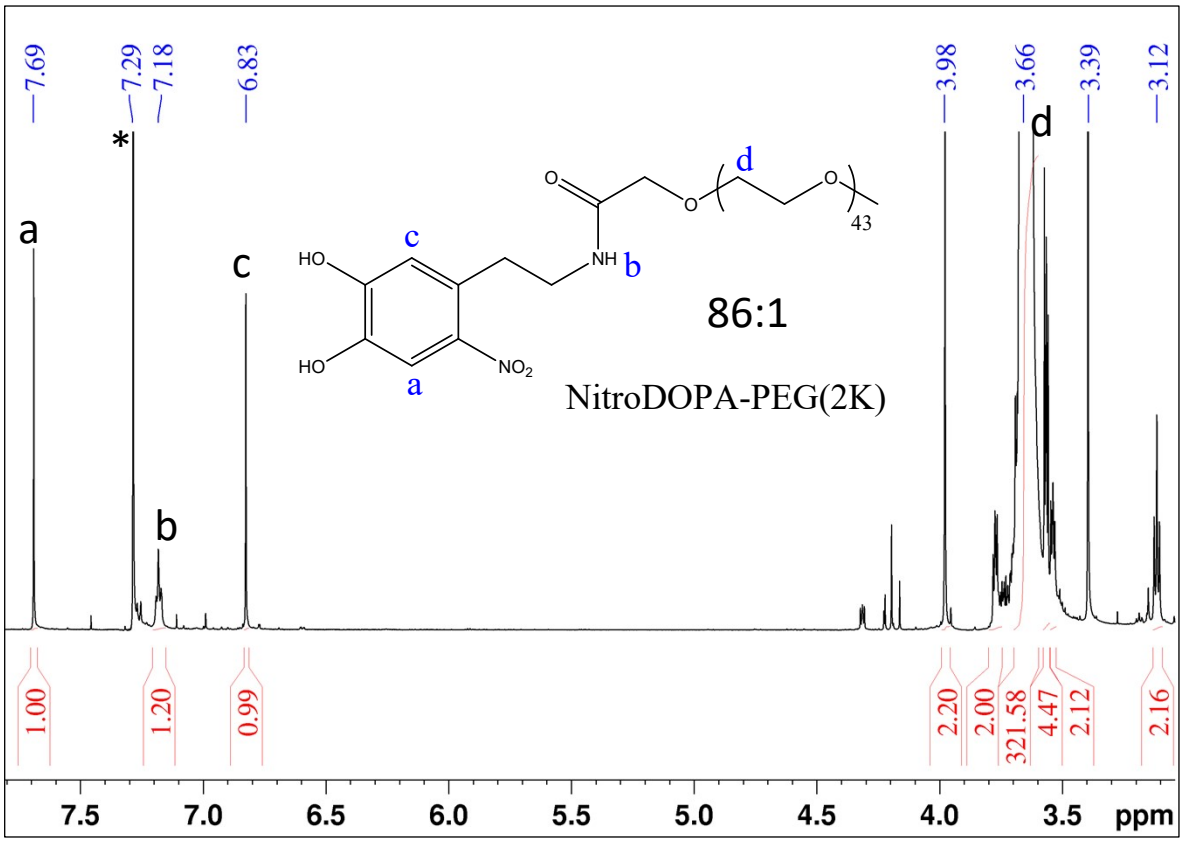

Figure S5. ^{1}H-NMR spectrum of ntroDOPA-PEG(2K) in $CDCl_3$. The peak(a) and peak(c) above 6.5 ppm represent protons on the dopamine aromatic ring. The largest peak(d) around 3.7 ppm represents protons on PEG chains. The peak labeled with (*) suggests $CDCl_3$ solvent residual peak. The ratio next to the molecular structure represents the ideal ratio between PEG protons and aromatic protons.

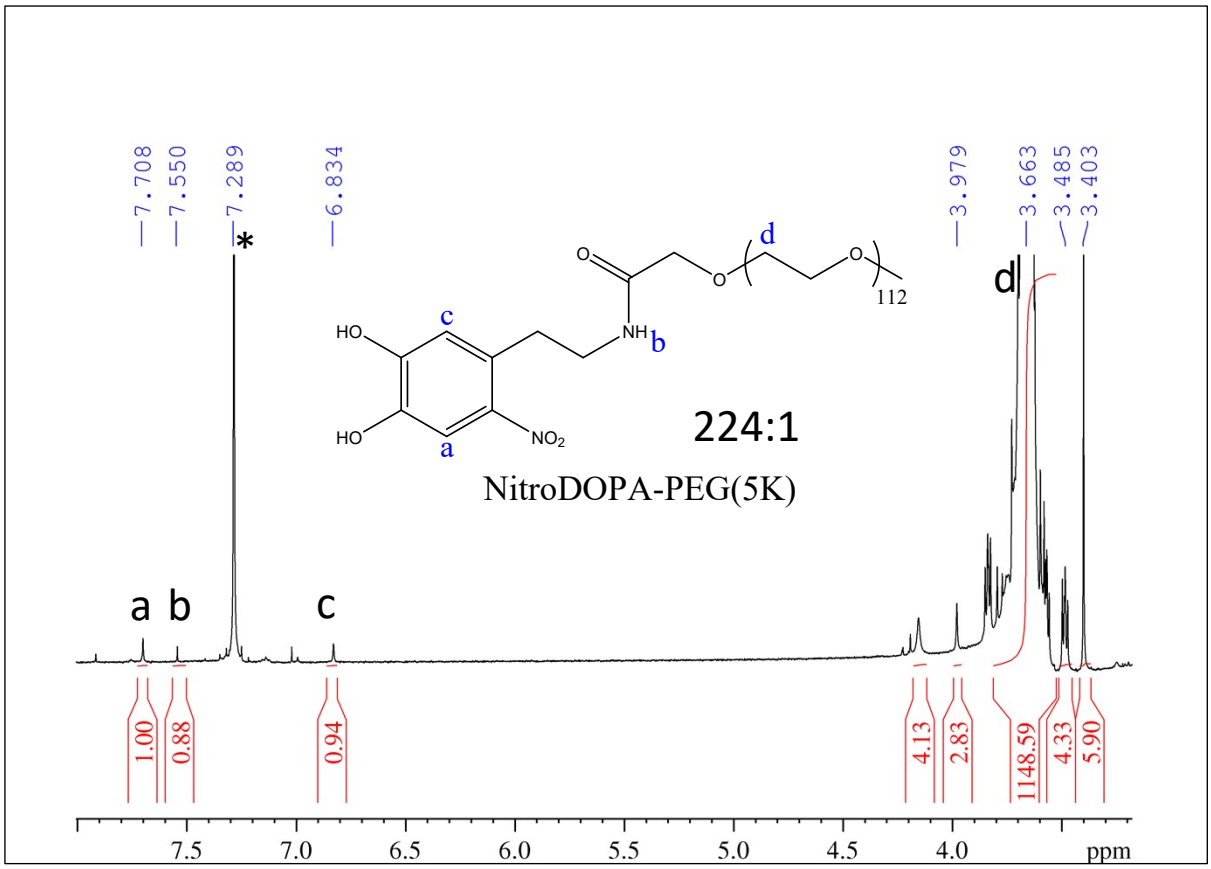

Figure S6. ^{1}H-NMR spectrum of nitroDOPA-PEG(5K) in $CDCl_3$. The peak(a) and peak(c) above 6.5 ppm represent protons on the dopamine aromatic ring. The largest peak(d) around 3.7 ppm represents protons on PEG chains. The peak labeled with (*) suggests $CDCl_3$ solvent residual peak. The ratio next to the molecular structure represents the ideal ratio between PEG protons and aromatic protons.

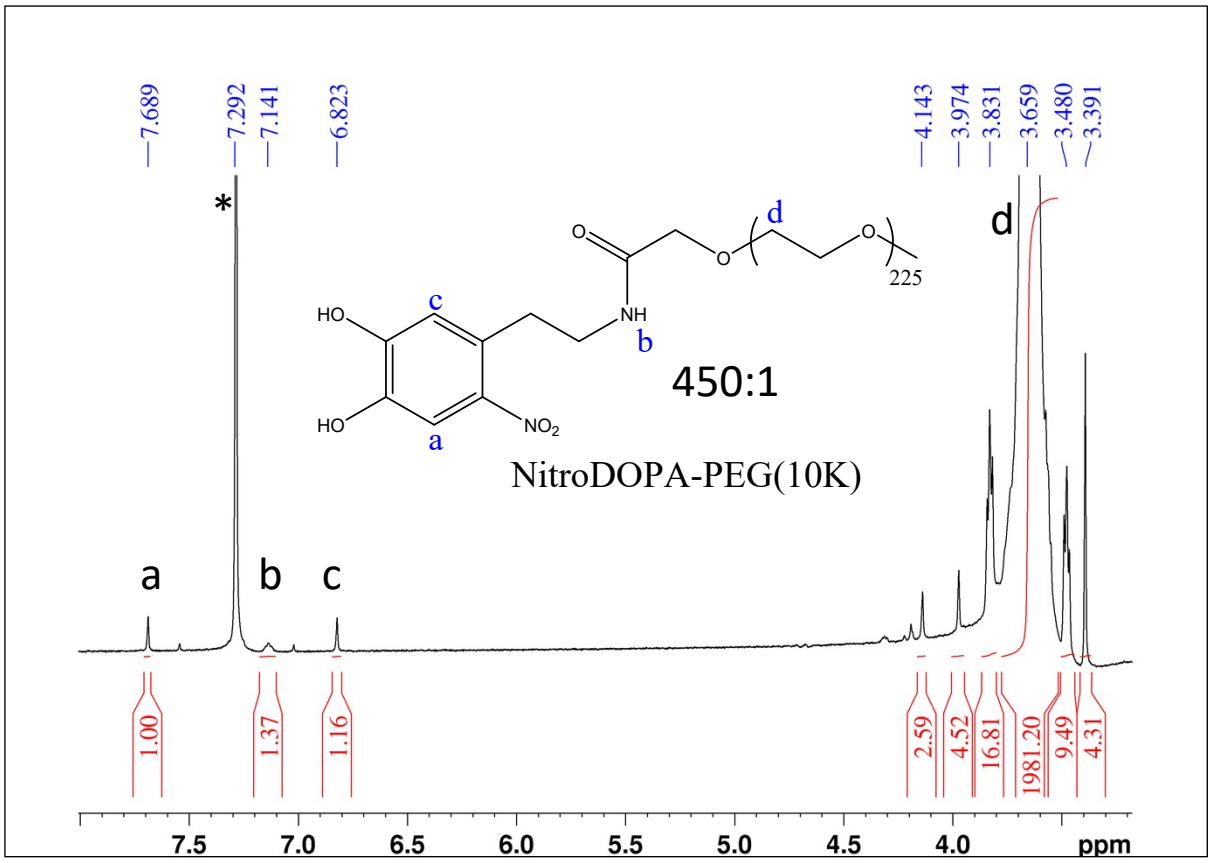

Figure S7. ^{1}H-NMR spectrum of nitroDOPA-PEG(10K) in $CDCl_3$. The peak(a) and peak(c) above 6.5 ppm represent protons on the dopamine aromatic ring. The largest peak(d) around 3.7 ppm represents protons on PEG chains. The peak labeled with (*) suggests $CDCl_3$ solvent residual peak. The ratio next to the molecular structure represents the ideal ratio between PEG protons and aromatic protons.

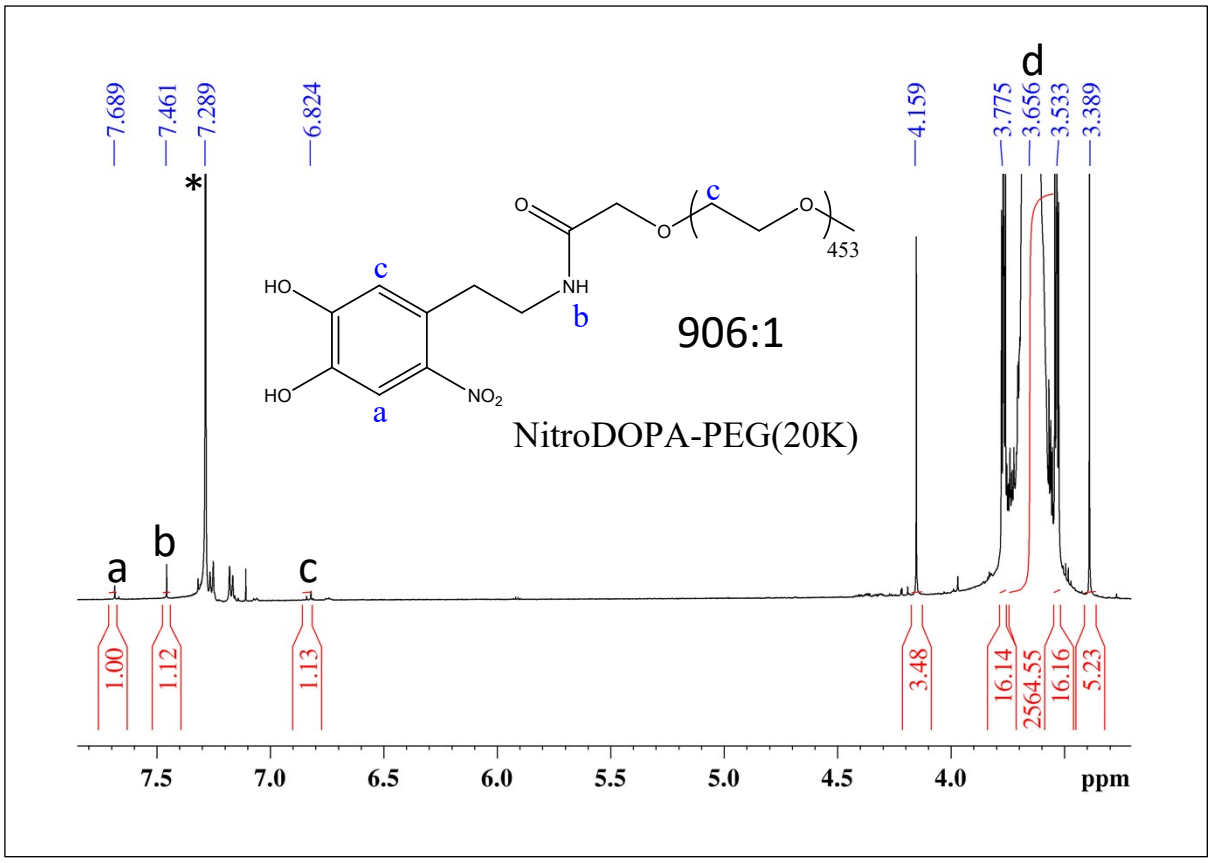

Figure S8. ^{1}H-NMR spectrum of nitroDOPA-PEG(20K) in $CDCl_3$. The peak(a) and peak(c) above 6.5 ppm represent protons on the dopamine aromatic ring. The largest peak(d) around 3.7 ppm represents protons on PEG chains. The peak labeled with (*) suggests $CDCl_3$ solvent residual peak. The ratio next to the molecular structure represents the ideal ratio between PEG protons and aromatic protons.

Table S3. Yield of nitroDOPA-PEG polymer crosslink reaction determined by ^{1}H-NMR spectra.

	NitroDOPA-PEG (2K)	NitroDOPA-PEG (5K)	NitroDOPA-PEG (10K)	NitroDOPA-PEG (20K)
Estimated proton ratio	86:1	224:1	450:1	906:1
Experiment proton ratio	161:1	574:1	990:1	1327:1
Yield	53.4%	39.0%	45.5%	68.3%

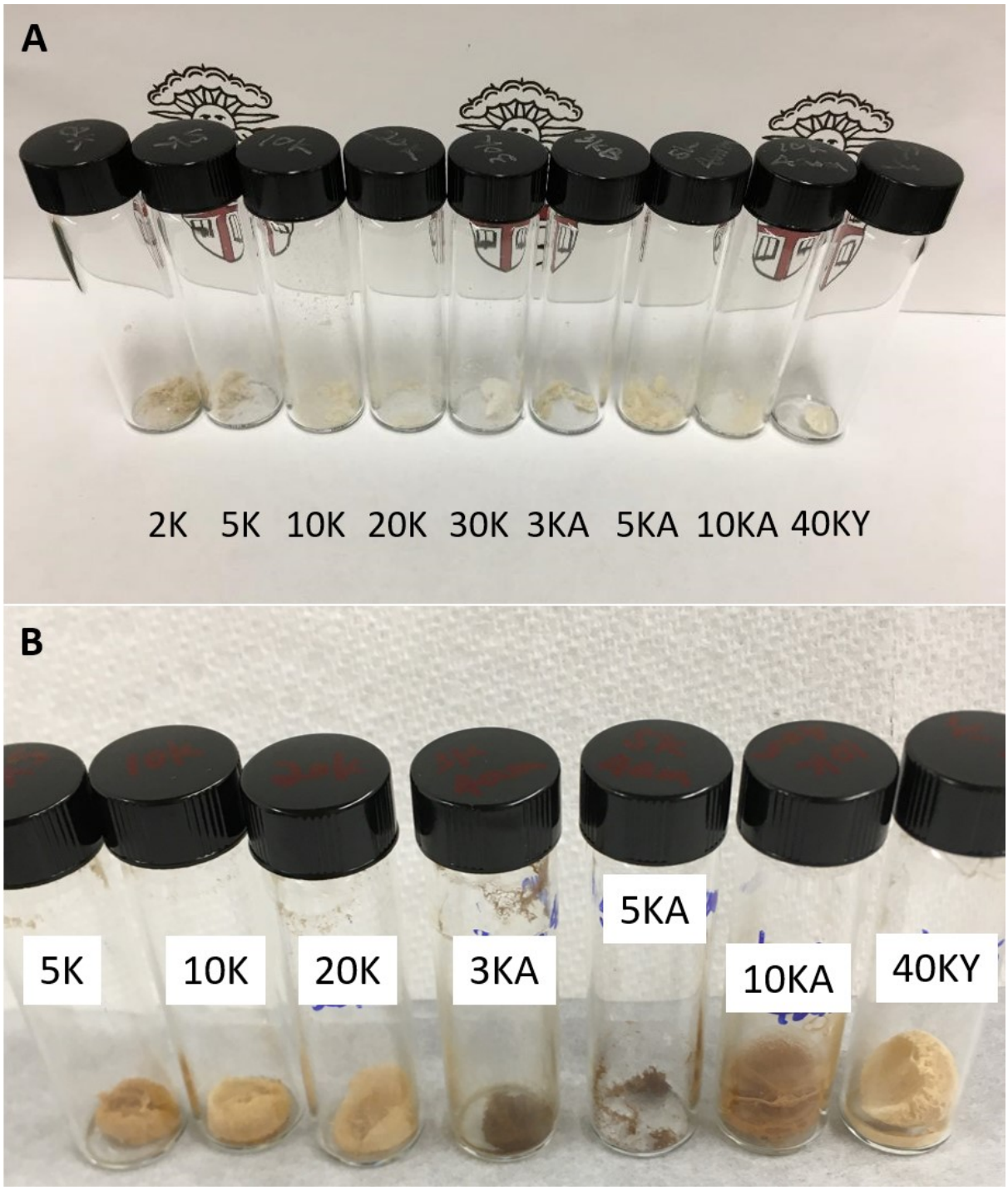

Figure S9. Photos of nitroDOPA-PEG polymers and nitroDOPA-PEG grafted ceria nanoparticles: (A) Photos of synthesized nitroDOPA-PEG polymer powders after dialysis and freeze-drying. (B) Photos of ceria nanoparticles coated with nitroDOPA-PEG after purification and freeze-drying. Polymers with a short PEG chain have a darker color.

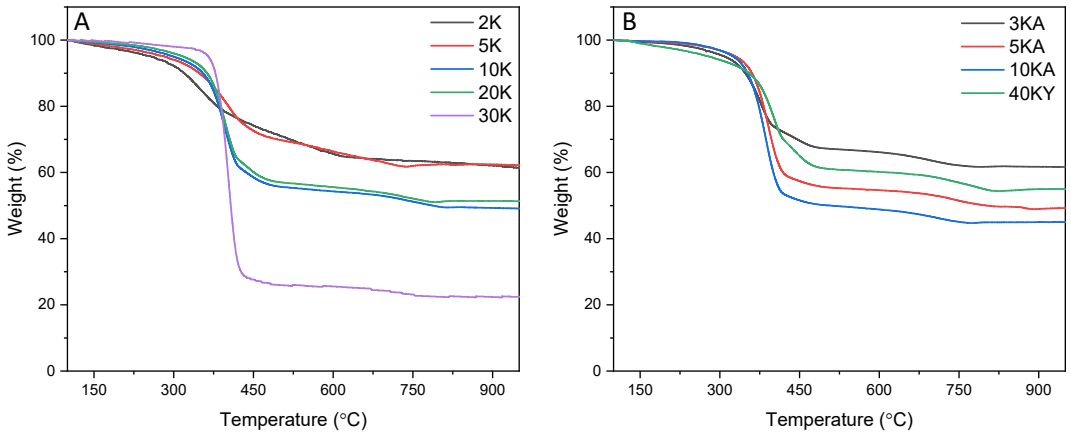

Figure S10. Thermogravimetric analysis (TGA) of ceria nanoparticle: linear (A) and branched (B) nitroDOPA-PEG-coated ceria nanoparticles in air. PEG polymer coatings decomposition completely over 450 ℃. Thermogravimetric analysis (TGA) was collected on the Mettler Toledo TG50 Thermogravimetric with an analyzer using an alumina crucible. All samples started with a mass at 1-3 mg. Samples were first heated to 90 ℃ and held for half an hour to get rid of the humidity. The heating rate of the analysis was 20 °C/min between 100 and 950 °C, under air atmosphere with a flow rate of 80 ml/min. All samples were tested three times.

Table S4. The grafting density and the number of polymer chains at the ceria particle interface. PEG polymers are classified into linear PEG and branched PEG.

PEG types	PEG MW (KDa))	Grafting Density (PEG/nm2)	std	Numbers of attached PEG chains	std
Linear PEG	2	1.25	0.00	98.5	0.3
	5	0.44	0.04	34.6	2.9
	10	0.37	0.04	29.2	3.4
	20	0.17	0.02	13.5	1.7
	30	0.17	0.01	13.3	0.6
Branched PEG	3	1.19	0.04	93.2	3.1
	5	0.70	0.09	55.2	6.7
	10	0.28	0.10	21.7	7.6
	40	0.15	0.09	11.9	7.0

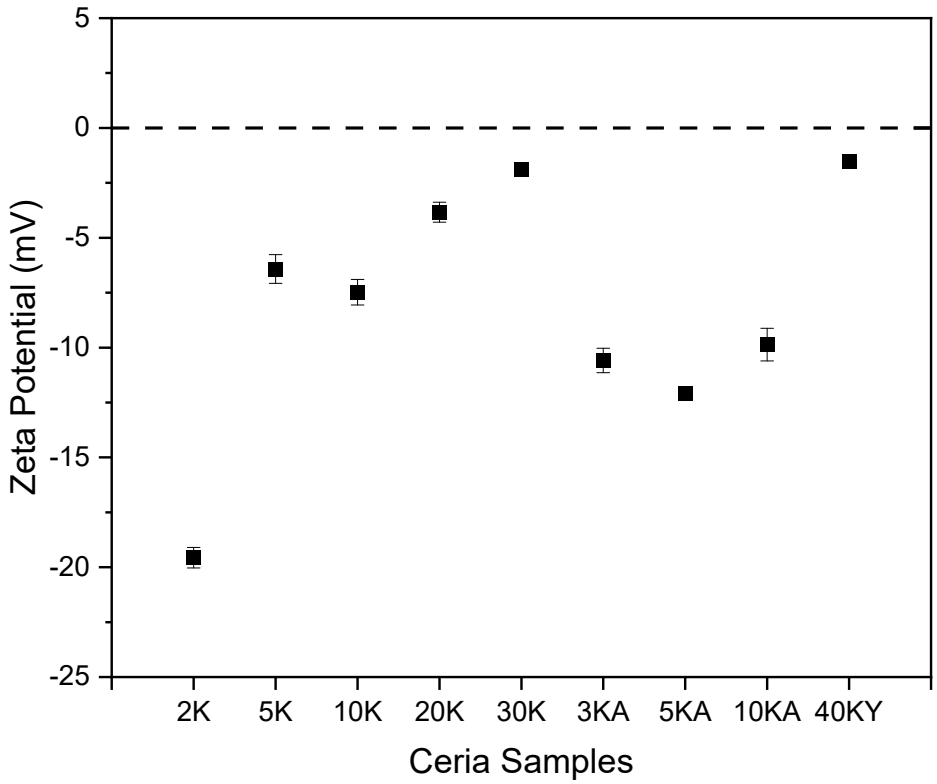

Figure S11. Zeta potential of ceria nanoparticles with different surface coatings.

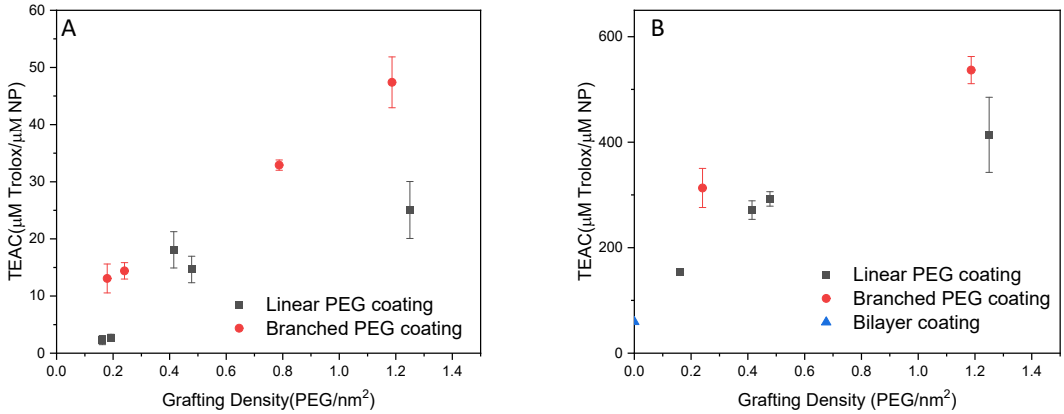

Figure S12. The Trolox equivalent antioxidant capacity (TEAC) of ceria nanoparticles with different coatings calculated from different antioxidant assays: Pyranie-TEAC assay(A), and Rhodamine-TEAC assay(B). Black dots represent linear PEG coatings, red dots represent branched PEG coatings, and the blue dot represents bilayer PEG (PEGPE) coating.

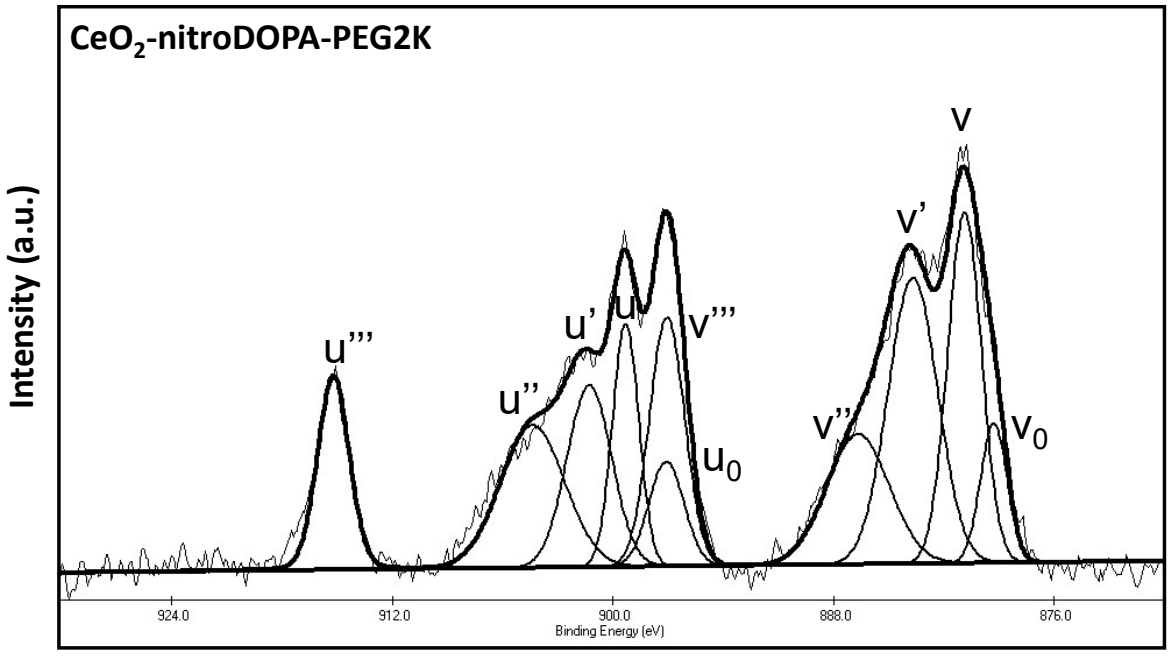

Peak Assignment	Origin of Ce contribute	Peak (eV)	FWHM (eV)	Area
u'''	Ce^{4+}	916.7	2	7429
u''	Ce^{4+}	905.9	4.1	10596.7
u'	Ce^{3+}	902.8	2.9	9400.1
u	Ce^{4+}	900.8	1.7	7417.6
u^0	Ce^{3+}	898.59	2.3	4271.5
v'''	Ce^{4+}	898.56	2.2	10097.5
v''	Ce^{4+}	888.2	4	9408.8
v'	Ce^{3+}	885.2	3.2	16409.5
v	Ce^{4+}	882.4	2.2	13675.4
v^0	Ce^{3+}	880.8	1.7	4295
Ce^{3+}(%)			36.96	

Figure S13. X-ray photoelectron spectra (XPS) of the Ce 3d region for CeO_2-nitroDOPA-PEG2K.

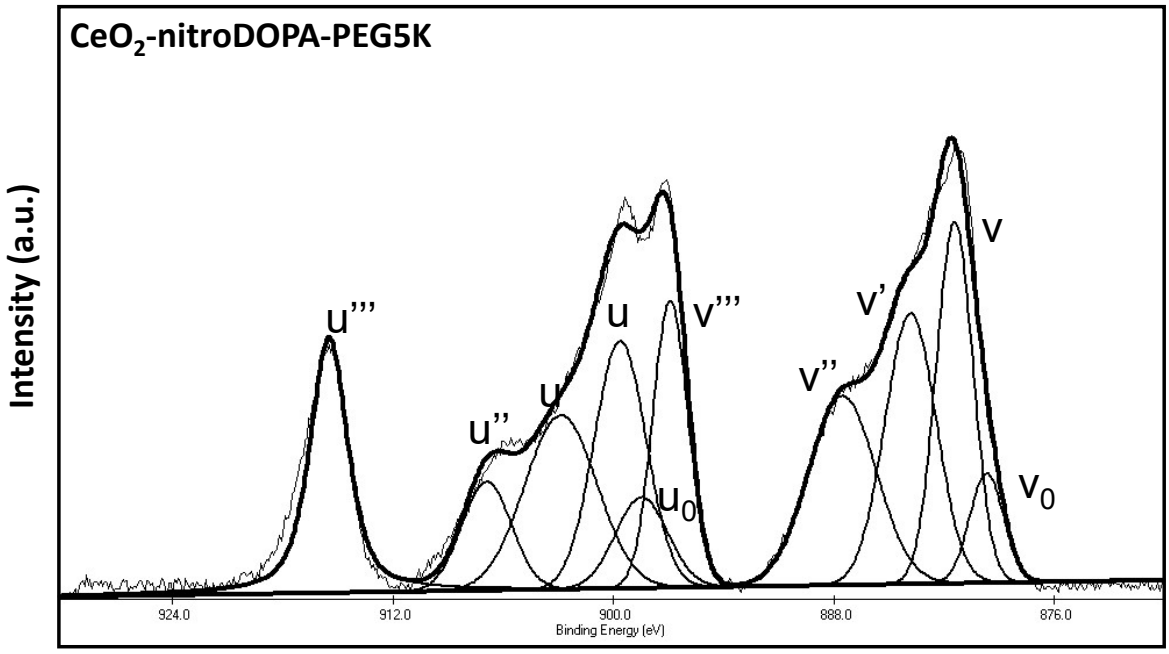

Peak Assignment	Origin of Ce contribute	Peak (eV)	FWHM (eV)	Area
u'''	Ce^{4+}	916.7	2.4	54563.4
u''	Ce^{4+}	908.1	3.2	23911.25
u'	Ce^{3+}	904.1	4.6	55565.9
u	Ce^{4+}	900.8	3.3	56791.9
u^0	Ce^{3+}	899.7	3.4	21116.5
v'''	Ce^{4+}	898.1	2.2	44535.2
v''	Ce^{4+}	888.7	4.3	56536.2
v'	Ce^{3+}	885	3.3	61228
v	Ce^{4+}	882.6	2.4	58753.9
v^0	Ce^{3+}	880.9	2.2	16500
Ce^{3+}(%)			34.35	

Figure S14. X-ray photoelectron spectra (XPS) of the Ce 3d region for CeO_2-nitroDOPA-PEG5K.

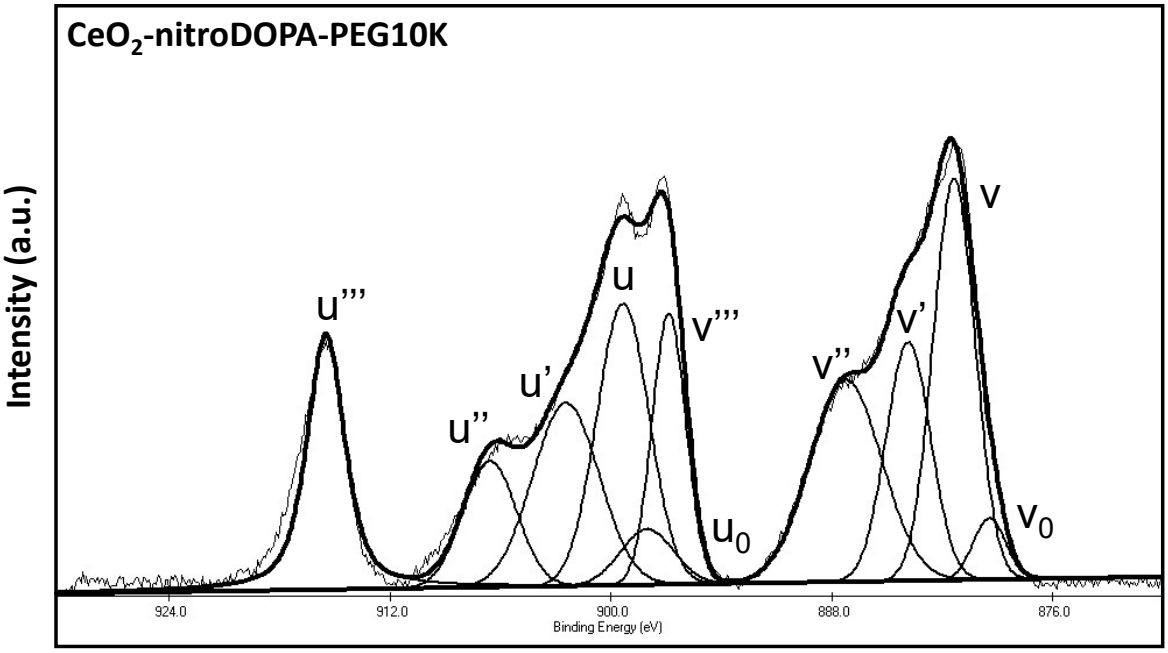

Peak Assignment	Origin of Ce contribute	Peak (eV)	FWHM (eV)	Area
u'''	Ce^{4+}	916.7	2.4	54504.8
u''	Ce^{4+}	907.8	3.4	29802.6
u'	Ce^{3+}	903.6	4.3	53716.6
u	Ce^{4+}	900.5	3.3	64865.3
u^0	Ce^{3+}	899.2	3.4	13105.2
v'''	Ce^{4+}	898.1	2.2	40262.1
v''	Ce^{4+}	888.4	4.6	63946.9
v'	Ce^{3+}	885.1	2.8	46889.9
v	Ce^{4+}	882.6	2.7	73778.5
v^0	Ce^{3+}	880.7	2.1	8833.8
	Ce^{3+}(%)		27.25	

Figure S15. X-ray photoelectron spectra (XPS) of the Ce 3d region for CeO_2-nitroDOPA-PEG10K.

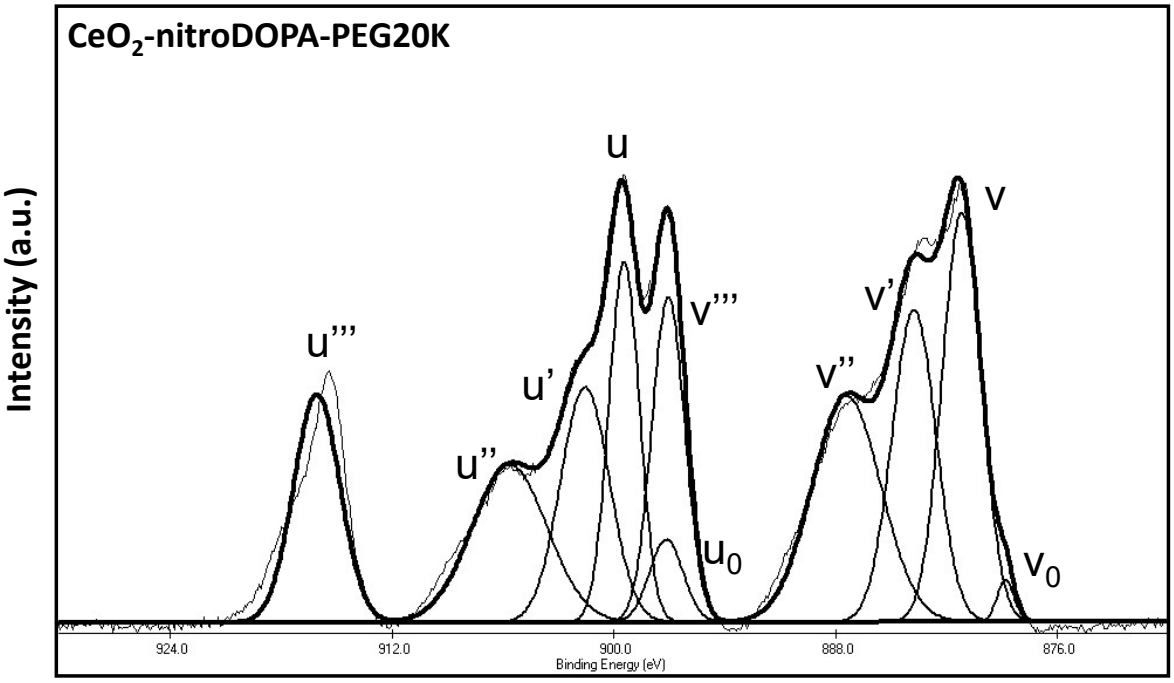

Peak Assignment	Origin of Ce contribute	Peak (eV)	FWHM (eV)	Area
u'''	Ce^{4+}	916.7	2.9	78866.2
u''	Ce^{4+}	906.2	4.8	88455.6
u'	Ce^{3+}	902.2	3.1	85772.7
u	Ce^{4+}	900.1	1.9	82242.5
u^0	Ce^{3+}	897.8	2.1	20800.0
v'''	Ce^{4+}	897.7	2.1	80058.0
v''	Ce^{4+}	888.0	4.4	116212.7
v'	Ce^{3+}	884.4	2.8	101933.3
v	Ce^{4+}	881.8	2.5	119883.9
v^0	Ce^{3+}	879.4	1.1	5312.6
	Ce^{3+}(%)		27.43	

Figure S16. X-ray photoelectron spectra (XPS) of the Ce 3d region for CeO_2-nitroDOPA-PEG20K.

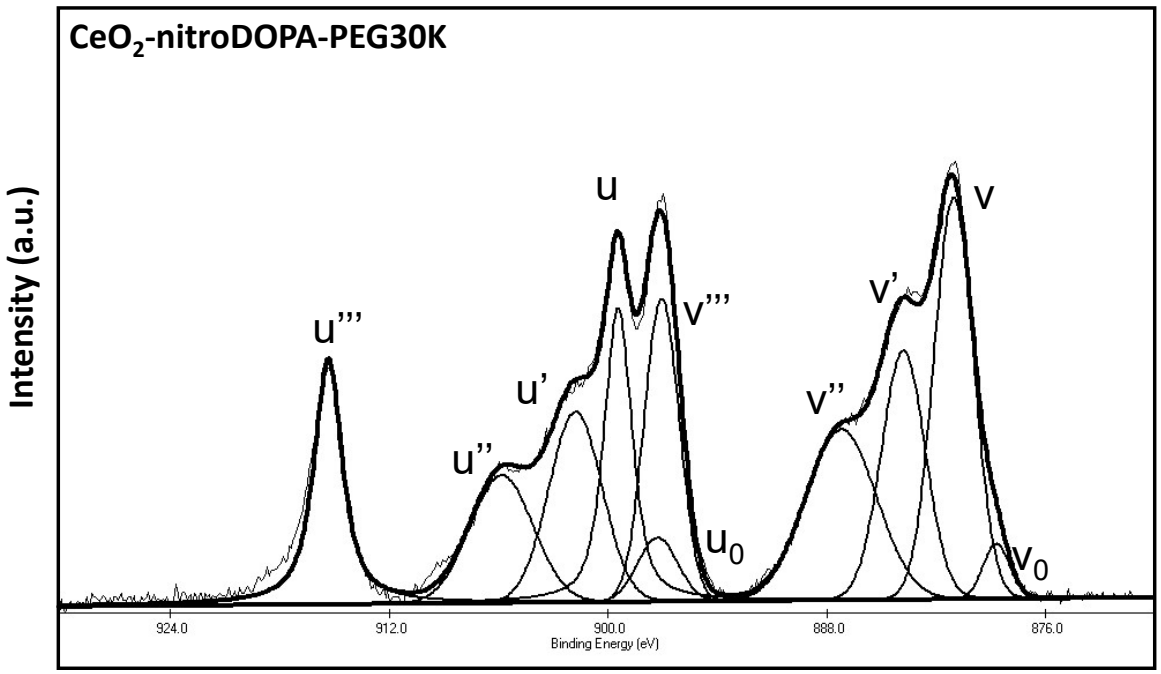

Peak Assignment	Origin of Ce contribute	Peak (eV)	FWHM (eV)	Area
u'''	Ce^{4+}	916.7	1.8	53825.7
u''	Ce^{4+}	907.2	4.1	45018.0
u'	Ce^{3+}	903.2	3.4	57171.7
u	Ce^{4+}	900.9	1.8	58578.5
u^0	Ce^{3+}	898.7	2.6	14426.7
v'''	Ce^{4+}	898.5	2.3	59487.1
v''	Ce^{4+}	888.6	4.5	67320.0
v'	Ce^{3+}	885.2	2.8	61818.2
v	Ce^{4+}	882.5	2.6	89576.7
v^0	Ce^{3+}	880.1	1.7	8249.8
Ce^{3+}(%)		27.48		

Figure S17. X-ray photoelectron spectra (XPS) of the Ce 3d region for CeO_2-nitroDOPA-PEG30K.

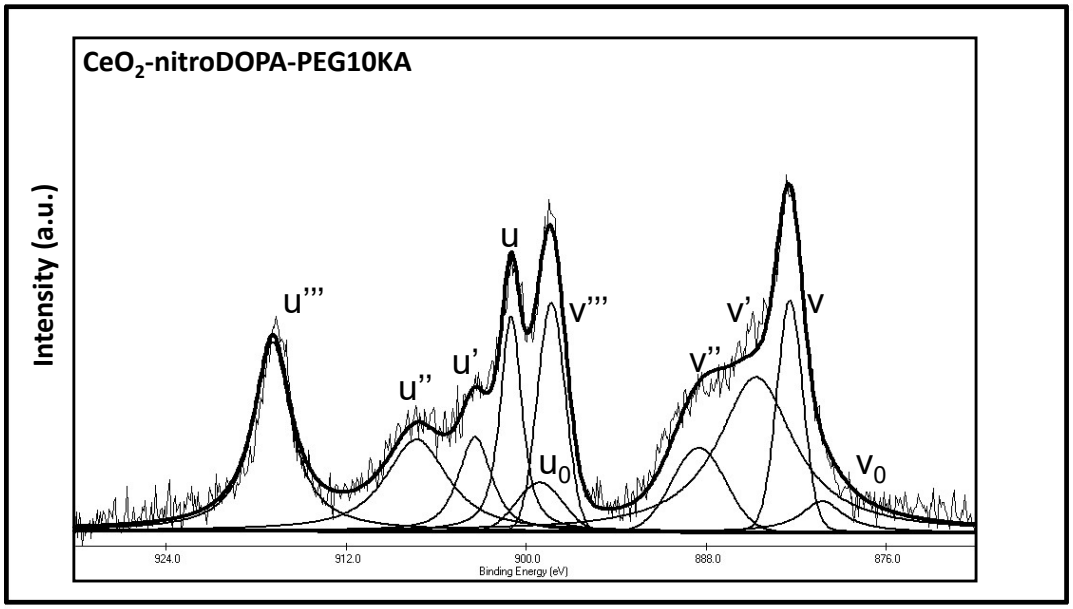

Peak Assignment	Origin of Ce contribute	Peak (eV)	FWHM (eV)	Area
u'''	Ce^{4+}	916.9	3.0	4746.2
u''	Ce^{4+}	907.3	5.0	3014.5
u'	Ce^{3+}	903.4	6.9	5455.5
u	Ce^{4+}	901.1	2.1	1903.9
u^0	Ce^{3+}	899.1	3.5	1100.0
v'''	Ce^{4+}	898.3	2.1	2847.1
v''	Ce^{4+}	888.5	4.2	2705.8
v'	Ce^{3+}	884.8	4.9	2900.7
v	Ce^{4+}	882.8	3.3	7802.6
v^0	Ce^{3+}	880.4	3.0	600.0
Ce^{3+}(%)			30.40	

Figure S18. X-ray photoelectron spectra (XPS) of the Ce 3d region for CeO_2-nitroDOPA-PEG10KA.

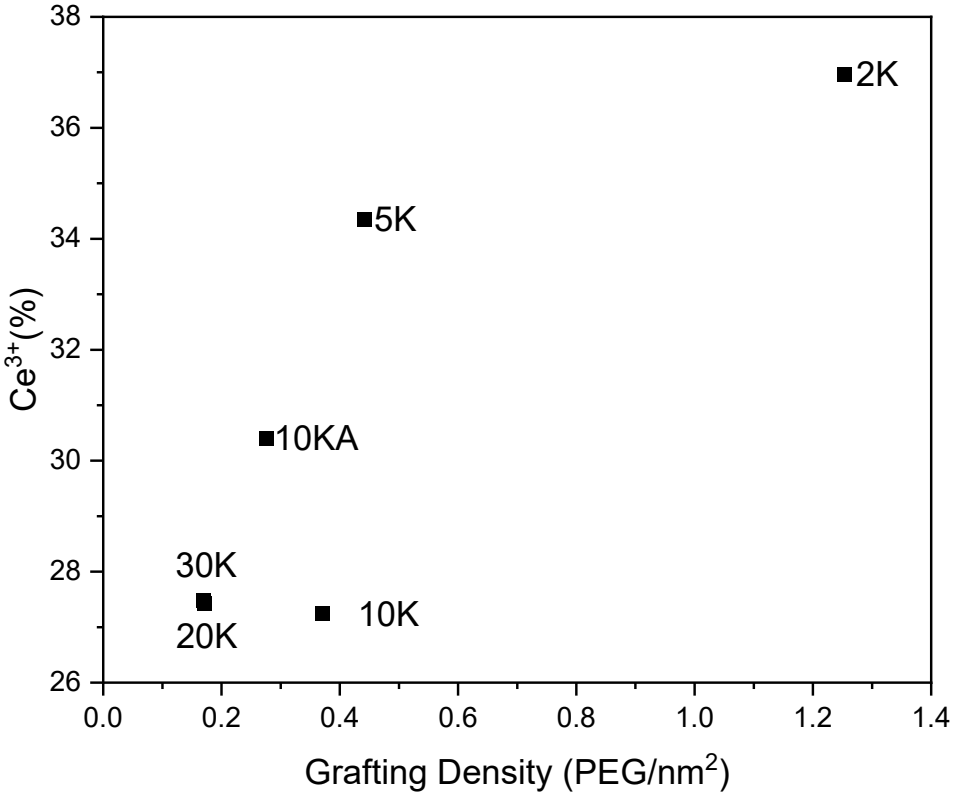

Figure S19. Ce(III) component calculated from XPS spectra increases with the increased grafting density of Ceria nanoparticles.